

Resonant cavity effect optimization of III-nitride thin-film flip-chip light-emitting diodes with microsphere arrays

PEIFEN ZHU^{1,2,4} AND NELSON TANSU^{1,3}

¹Department of Electrical and Computer Engineering, Center for Photonics and Nanoelectronics, Lehigh University, Bethlehem, Pennsylvania 18015, USA

²Department of Physics and Engineering Physics, The University of Tulsa, 800 South Tucker Drive, Tulsa, Oklahoma 74104, USA

³e-mail: tansu@lehigh.edu

⁴e-mail: pez311@lehigh.edu

Received 11 May 2015; accepted 15 June 2015; posted 19 June 2015 (Doc. ID 240584); published 8 July 2015

Comprehensive studies were carried out to investigate the light extraction efficiency of thin-film flip-chip (TFFC) light-emitting diodes (LEDs) with anatase TiO₂ microsphere arrays by employing the finite-difference time-domain method. The quantum well position and the resonant cavity effect were studied to obtain optimum light extraction for the planar TFFC LED. Further enhancement in light extraction was achieved by depositing microsphere arrays on the TFFC LED. The calculation results showed that the sphere diameter, packing density, and packing configuration have significant effects on the light extraction efficiency. A maximum light extraction efficiency of 75% in TFFC LEDs with microsphere arrays has been achieved. This study demonstrates the importance of optimizing the quantum well position, cavity thickness, sphere diameter, sphere packing density, and packing configuration for enhancing the light extraction efficiency of TFFC LEDs with microsphere arrays. © 2015 Optical Society of America

OCIS codes: (230.3670) Light-emitting diodes; (250.0250) Optoelectronics.

<http://dx.doi.org/10.1364/AO.54.006305>

1. INTRODUCTION

The development of GaN-based semiconductors can be traced back to the early work at RCA Laboratories in 1969 [1]. Since then, tremendous efforts have been devoted to the growth of wurtzite GaN and InGaN, the control of the p-GaN conductivity, and the development of LED technologies [2–6]. However, one of the major challenges for GaN-based LEDs is the poor electrical conductivity of p-GaN [7,8]. This leads to challenges related to the current spreading underneath p-electrode, which results in nonhomogeneous light emission from the LED chip. This problem can be solved by the deposition of a semi-transparent Ni/Au layer on the p-GaN [9,10], which overcomes the current spreading problem. However, the light extraction efficiency of the LED is reduced due to the absorption of the Ni/Au layer. The LED performance is thus a tradeoff between optimized current spreading uniformity and light extraction. Specifically, thicker Ni/Au can improve the current spreading in p-GaN but reduces the light extraction efficiency significantly while a thinner Ni/Au layer can improve the light extraction efficiency but at the cost of efficient current spreading.

In order to eliminate the light absorption of the semi-transparent metal while keeping good current spreading,

flip-chip technology is implemented in LED devices [11]. In this approach, the thick Ni/Au metal is deposited on the p-GaN and the light is extracted from the sapphire substrate. However, the refractive index of GaN and sapphire are 2.5 and 1.8 respectively, which are much larger than the refractive index of free space. According to Snell's law, strong reflection at both the n-GaN-sapphire boundary and the boundary between the sapphire and free space will result in light trapping within the n-GaN layer and sapphire substrate. In order to extract the guided modes out of the devices, the laser-liftoff method is applied to the LED device to remove the sapphire substrate followed by thinning down the n-GaN, resulting in a thin-film flip chip (TFFC) structure [12]. In this device configuration, the interference effect was used to enhance the light extraction, and maximum light extraction efficiency of 27% has been achieved by tuning the p-GaN thickness and cavity thickness [13–16]. Further enhancement in light extraction efficiency was achieved via surface modification of the TFFC LED by employing nanostructures. The use of surface roughness and photonic crystals are the two most effective approaches, which result in light extraction of 65% and 72%, respectively [13,17]. The use of dry-etched GaN nanostructures had also been

investigated as an approach to achieve improved extraction in TFCC LEDs [18–20]. However, the nonuniformity of surface roughness and high cost of photonic crystals are hindering the wide adoption of LED in the illumination market. The use of cost-effective methods to enhance the light extraction of TFCC LEDs is instrumental in pushing LED implementation today in solid-state lighting.

Our recent works demonstrated the implementation of SiO_2 and TiO_2 sphere arrays and microlens arrays on the conventional top-emitting GaN-based LED. The microsphere and microlens arrays were deposited by the cost-effective rapid convective deposition method [21–23], and resulted in significant enhancement in light extraction efficiency [22–26]. The importance of sphere refractive index and diameter on the light extraction efficiency was discussed in our previous work [26]. The microlens arrays were also employed as an imprinting template for a fabricating concave structure on a GaN-based LED and corrugated structures in an organic LED (OLED), which resulted in ~ 3 times enhancement in power efficiency [27,28]. Our recent work has also shown the ability to engineer hexagonal or square lattice arrays using this method [21,29], as well as the importance of having hexagonal close-packed lattice arrays as the optimum structure for light extraction purposes [29].

In this work, a comprehensive study was carried out to optimize TFCC LEDs with microsphere arrays. The goal of this study is to investigate how much improvement in term of absolute extraction efficiency can be achieved from the implementation of microsphere array techniques on TFCC LEDs. This study provides useful guidance for potential implementation in industry by taking the microsphere array deposition method and translating that into TFCC LED integration. The optimization of the LED extraction efficiency was performed in TFCC LED device configuration by taking into account the cavity effect, microsphere properties, sphere diameters, p-GaN thickness, and periodical arrangement of microsphere arrays.

2. FDTD ANALYSIS OF LIGHT EXTRACTION EFFICIENCY FOR TFCC LEDs

The finite-difference time-domain (FDTD) method [26] was employed to calculate the light extraction efficiency of TFCC LEDs. The TFCC LED device structure analyzed in this study is shown in Fig. 1. An InGaN/GaN quantum well is sandwiched by p-GaN and n-GaN, and the refractive index of

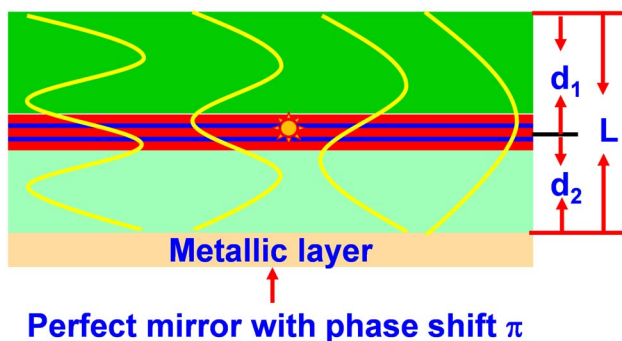


Fig. 1. Schematic of TFCC LEDs used in FDTD simulation with quantum well positioning within the structure.

GaN was set to 2.5. The metallic mirror was attached to the bottom of the LED, which is assumed to be a perfect mirror with 100% reflectance. Considering the computational efficiency in FDTD simulation, we employed a simulation domain of $10 \mu\text{m} \times 10 \mu\text{m}$ with perfect matched layer boundary conditions applied to the lateral boundaries and perfect electric conductor (PEC) boundary conditions applied to the bottom of the LED. The grid size was set to be 10 nm to ensure accurate results. The simulation time was set to be large enough to make sure of the stabilized field output.

One dipole was chosen as the light source within the quantum well region and positioned in the center region of the quantum well. The emission wavelength used in this calculation was set to $\lambda = 500 \text{ nm}$. The light extraction efficiency was calculated as the ratio of the optical output power extracted from the top of the LED to the total output power generated by the dipole. The details of the FDTD simulation method were described previously in our recent work [26].

3. LIGHT EXTRACTION OF TFCC PLANAR LEDs: QUANTUM WELL POSITION AND RESONANT CAVITY EFFECT

The conventional LED structure can be grown on the sapphire substrate; then the TFCC LED can be fabricated via the laser-lift-off process to remove the sapphire substrate, followed by chemical-mechanical polishing (CMP) to thin down the n-GaN, which results in a TFCC LED with tunable n-GaN thickness [30]. Note that the p-GaN thickness can be tuned in the epitaxy process. Thus, a TFCC LED structure with various p-GaN and n-GaN thicknesses can be achieved by tuning epitaxy growth and CMP times.

As shown in Fig. 1, the metal contact below the p-GaN in the TFCC LED reflects the downward-traveling light, which leads to the interference of light between the upward-traveling light and the reflected light. In addition, a fraction of the upward-traveling light will be reflected back to the active region at the interface of the GaN and free space, which will lead to interference as well. Therefore, proper design of quantum well position as well as the cavity thickness of the LED structure will have a significant effect on the light extraction efficiency [15,16,31–40].

The cavity thickness and quantum well position, determined by the p-GaN thickness, were tuned to obtain the maximum light extraction efficiency. The optimized planar TFCC LED structure will be used as reference for the TFCC LED with microspheres. In this calculation, the cavity thickness was chosen as 700 nm and the p-GaN thickness was tuned to investigate the effect of quantum well position on the light extraction efficiency of TFCC LEDs.

Figure 2 shows the light extraction efficiency of TFCC LEDs ($\lambda = 500 \text{ nm}$) with a cavity thickness of 700 nm. The extraction efficiency of the LEDs shows a strong dependency on the p-GaN thickness. The higher efficiencies were achieved at p-GaN thicknesses of 50, 150, 250, and 350 nm; the lower efficiencies were observed at p-GaN thickness of 100, 200, and 300 nm. This finding shown here is consistent with the interference theory.

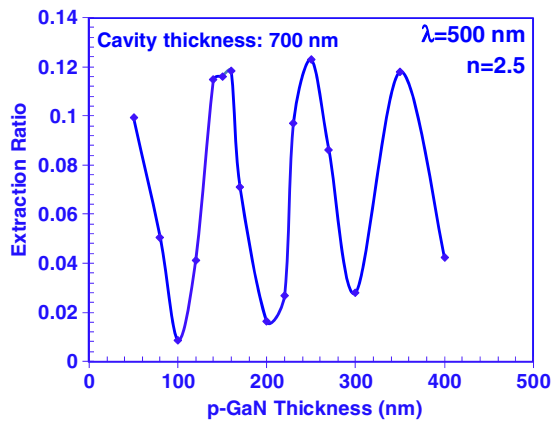


Fig. 2. Quantum well position-dependent light extraction efficiency of TFFC LEDs with cavity thickness of 700 nm.

In order to investigate the resonant cavity effect on the light extraction efficiency, the light extraction of LEDs with various cavity thicknesses was also calculated with a constant p-GaN thickness of 150 nm (Fig. 3). The thickness of p-GaN was

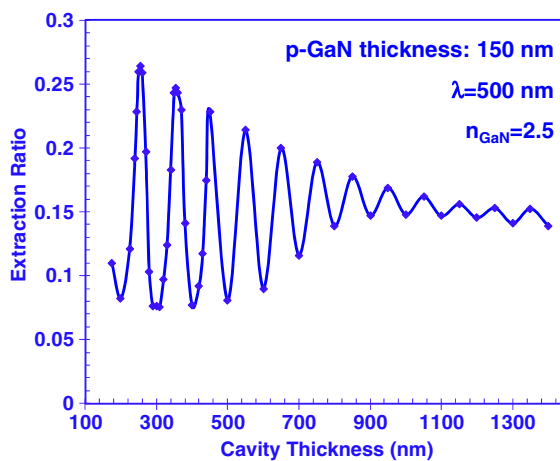


Fig. 3. Light extraction efficiency of TFFC LEDs with various cavity thicknesses for the p-GaN thickness of 150 nm.

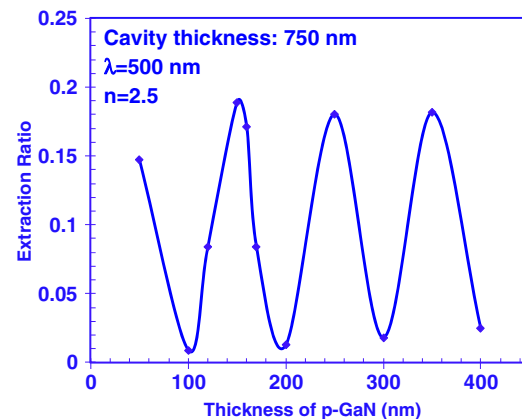
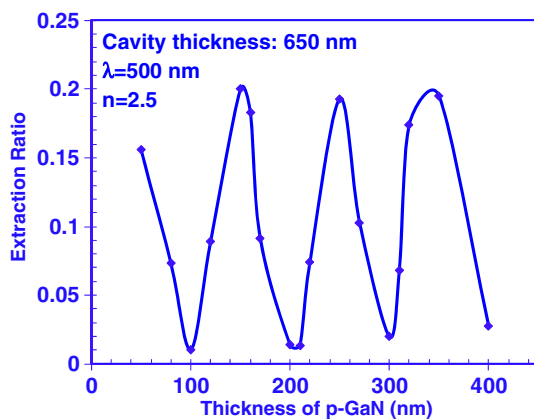


Fig. 4. Quantum well position-dependent light extraction efficiency of TFFC LEDs with cavity thickness of 600 nm (left) and 750 nm (right).

chosen as 150 nm, which is the optimized p-GaN thickness in typical TFFC LEDs. As shown in Fig. 3, the periodic modulation of the extraction efficiency with varying cavity thicknesses is observed, which is attributed to the interference effect of multiple light reflections inside the LED. An extraction efficiency of $\sim 27\%$ is achieved for cavity thickness of 250 nm, which is a $\sim 6-7$ times improvement over the conventional top-emitting LED devices. The modulation depth decreases as the cavity thickness increases. For small cavity thickness, only a small number of the Fabry–Perot modes exist, resulting in higher extraction efficiency. The Fabry–Perot modes increase with cavity thickness, which leads to the averaging of the many modes and a weaker interference effect.

From our previous calculation, the light extraction efficiency reaches a maximum at cavity thicknesses of 250, 350, 450, 550, 650, and 750 nm. However, the maximum extraction efficiency decreases with the increase in the cavity thickness. Our analysis focuses on the cavity thicknesses of 650 and 750 nm, as these structures are experimentally implementable and have reasonable light extraction efficiency. Thus, we further optimized quantum well position for the LED with cavity thickness of 650 and 750 nm for optimizing the light extraction efficiency. Figure 4 shows the light extraction efficiency as a function of quantum well position for TFFC LEDs with cavity thicknesses of 650 and 750 nm. Maximum light extraction efficiencies of 20% and 19% were achieved at p-GaN thickness of 150 nm for LEDs with cavity thicknesses of 650 nm and 750 nm, respectively.

4. EXTRACTION EFFICIENCY OF TFFC LEDs WITH MICROSPHERE ARRAYS

The light extraction efficiency of the TFFC LEDs measured is much higher than that of conventional top-emitting LEDs, but further low-cost improvement approaches to external quantum efficiency are necessary to increase the market penetration of this technology. Further optimization could be achieved by depositing TiO_2 sphere arrays onto the TFFC LED, which is similar to the reported approach on the conventional LED [26].

As reported in a previous work [41], the fabrication of TiO_2 microsphere arrays on top of the LED can be performed via the rapid convective deposition (RCD) method. RCD is a

self-assembly process which deposits negative-charged particles under the capillary force. By modifying the deposition speed (v_d), different packing densities (i.e., submonolayer, monolayer, and multilayer) can be obtained. The critical speed for achieving monolayer is determined by evaporation rate, volume fraction of microsphere suspension, porosity of the colloidal crystal, and the height of thin film. Note that by tuning the porosity of the colloidal crystal, different packing geometries (i.e., hexagonal close-packed array and square close-packed array) can be obtained. The microsphere arrays with different packing densities and packing geometries are illustrated in Fig. 5. Note that monodisperse TiO_2 spheres can be synthesized by the mixed-solvent method [42], and the diameter of the spheres can also be engineered by tuning the concentrations of ethanol and acetonitrile.

Detailed analysis on the effect of the microsphere arrays on TFFC LEDs has been performed focusing on sphere packing geometry, sphere packing density, and sphere diameter. Due to the matched refractive index between the TiO_2 microsphere arrays and the GaN layer, TiO_2 microsphere arrays show enhanced performance over the SiO_2 microsphere arrays [22]. Therefore, the study of microsphere arrays and their effects on the performance of TFFC LEDs will focus on the TiO_2 sphere arrays.

First, the effects of the microsphere array packing geometries on the light extraction of TFFC LEDs are compared. Figure 6 shows a comparison of the far-field radiation patterns for the planar LED (as reference), and LEDs with hexagonal close-packed geometry and square close-packed geometry. The far-field radiation patterns show that significantly enhanced light extraction in larger angular direction was observed for the LED with hexagonal close-packed monolayer sphere arrays. The enhanced light extraction of the LED with square close-packed sphere arrays is also observed both in the large angular and normal directions. However, the far-field intensities exhibit different symmetries: a hexagonal pattern for the microsphere LED with a hexagonal close-packed structure, and a square

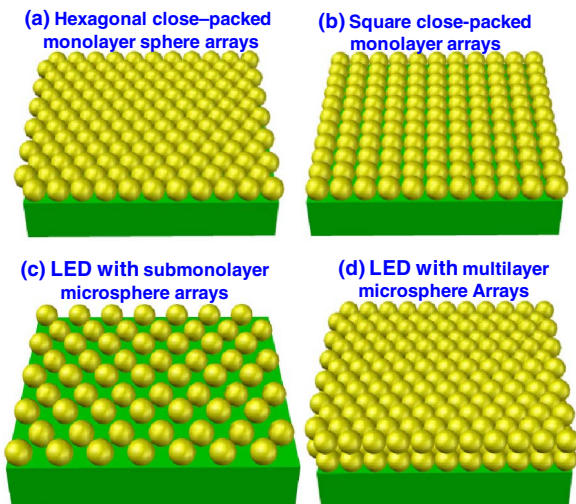


Fig. 5. Schematic of microsphere LEDs with (a) hexagonal close-packed sphere arrays, (b) square close-packed sphere arrays, (c) submonolayer sphere arrays, and (d) multilayer microsphere arrays.

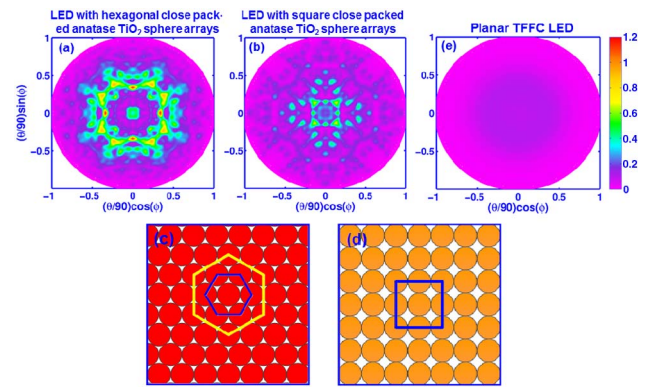


Fig. 6. Far-field radiation pattern of microsphere TFFC LEDs with different packing geometry: (a) with hexagonal close-packed geometry shown as (c); (b) with square close-packed geometry shown as (d); and (e) planar LED.

radiation pattern for the microsphere array LED with a square close-packed symmetry. This indicates that the sphere array arrangement has a significant effect on light scattering, resulting in notable change in the far-field radiation pattern. Comparison of the radiation patterns shows that the LED with a hexagonal close-packed monolayer sphere array exhibits higher output power intensity than the LED with a square close-packed sphere array. Therefore, our following analysis will mainly focus on the TFFC LED with hexagonal close-packed microsphere arrays.

In addition to the microsphere array packing geometry, the packing density of the microsphere array could also have a notable effect on the light extraction of LEDs. Figure 7 shows the comparison of the far-field radiation patterns between the planar LED, LEDs with submonolayer sphere arrays, LEDs with monolayer sphere arrays, and LEDs with multilayer sphere arrays. The far-field radiation pattern for the planar LEDs [as shown in Fig. 6(e)] exhibits a Lambertian radiation pattern with only angular dependency and symmetrically azimuthal distribution. The far-field intensity is much weaker in all angular directions compared to the microsphere LEDs due to the narrower light escape, and only a small fraction of light is extracted out from the LED device. The inner and outer radiation rings are attributed to the direct emission from the InGaN quantum wells (QWs) and reflected emission by PEC reflectors, respectively. The LEDs with microsphere arrays exhibit both angular and azimuthal dependency as shown in Figs. 7(a)–7(f). Significantly higher intensity is observed for the far-field radiation patterns of microsphere array LEDs in the normal and large angular distributions, which in turn results in improved light extraction efficiency for these LEDs. The far-field intensity of LEDs with microsphere arrays exhibits hexagonal symmetry due to the hexagonal packed nature of sphere arrays. However, the light distribution along the angular and azimuthal directions differs for the LEDs with submonolayer sphere arrays, monolayer arrays, and multilayer arrays. For the LED with monolayer microsphere arrays, most of the light was extracted out in the larger angular direction, which resulted in enhanced light extraction efficiency, while only a small amount of light was extracted out in the smaller angular

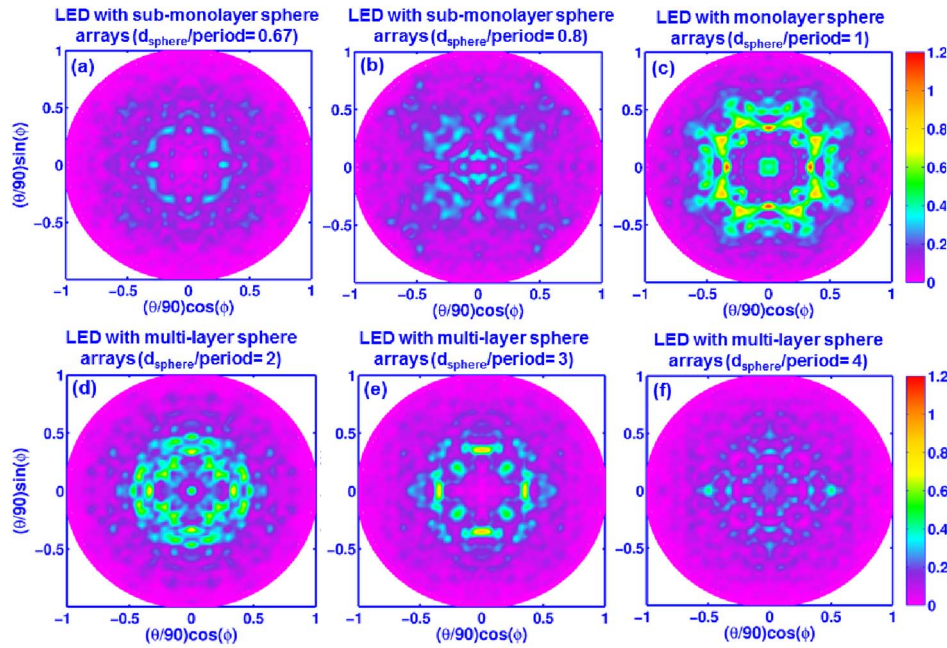


Fig. 7. Far-field radiation pattern of microsphere TFFC LEDs with submonolayer, monolayer, and multilayer sphere arrays with packing densities of (a) 0.67, (b) 0.8, (c) 1, (d) 2, (e) 3, and (f) 4.

direction. For the case of LEDs with submonolayer sphere arrays, the light is spread over a larger surface and it can be extracted out in a relatively larger angular range; however, the overall intensity is lower than that of LEDs with monolayer sphere arrays. The same phenomenon is observed for LEDs with multilayer sphere arrays, but the light intensity is much lower than that of LEDs with monolayer sphere arrays.

Next, the effect of the microsphere diameter on the light extraction efficiency of TFFC LEDs is examined. Figure 8 shows the light extraction efficiencies of microsphere array TFFC LEDs with diameters of 250, 400, 500, 600, 750, 850, and 1 μm . The light extraction efficiency changes with the diameter of the microspheres. Extraction efficiencies of 39%, 63%, 38%, 28%, 53%, 46%, and 27% were achieved

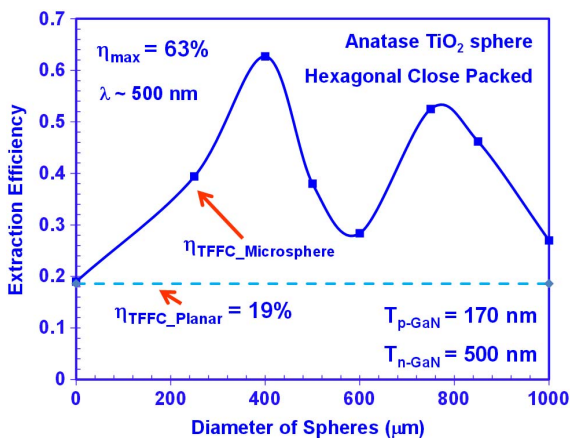


Fig. 8. Light extraction efficiency of microsphere LED with microsphere arrays.

for TFFC LEDs with sphere diameters of 250 nm, 400 nm, 500 nm, 600 nm, 750 nm, 850 nm, and 1 μm , respectively. Note that only 20% of light can be extracted out for the planar TFFC LED with the same cavity thickness and quantum well position. The light extraction efficiency is significantly enhanced by the use of TiO_2 microsphere arrays on the LED surface, leading to a wider light escape cone due to the curved boundary between the spheres and free space. Note that the diameter of the sphere has a significant effect on the light extraction efficiency of the LEDs. The LED with the 400 nm sphere shows an extraction efficiency of 63%. When the light collides with the TiO_2 sphere with size comparable to its wavelength, the light scatters strongly along the forward direction. This effect enhances the light extraction. Note that the comparison of light extraction efficiency between microsphere array LEDs and planar LEDs was carried out by taking the total output power integrated over the whole solid angle.

The light extraction efficiency of TFFC LEDs with microspheres was further optimized by engineering the cavity thickness. The p-GaN thickness was chosen as 170 nm, which is within a typical range for the p-type layer thickness in LED epitaxy. The cavity thickness was tuned from 640 to 700 nm. Figure 9 shows the light extraction efficiency of TFFC LEDs with various cavity thicknesses. Extraction efficiencies of 46%, 59%, 74%, 62.7%, 59%, and 50% were achieved for cavity thicknesses of 643 nm, 653 nm, 663 nm, 673 nm, 678 nm, and 683 nm, respectively. The efficiency varies from 42% to 62.7%. The modulation of extraction efficiency with various cavity thicknesses is attributed to the interference of multiple reflections in the Fabry–Perot cavity structure. An extraction efficiency of 63% is achieved for a cavity thickness of 673 nm, which is a ~ 16 times improvement over that of a conventional top-emitting LED.

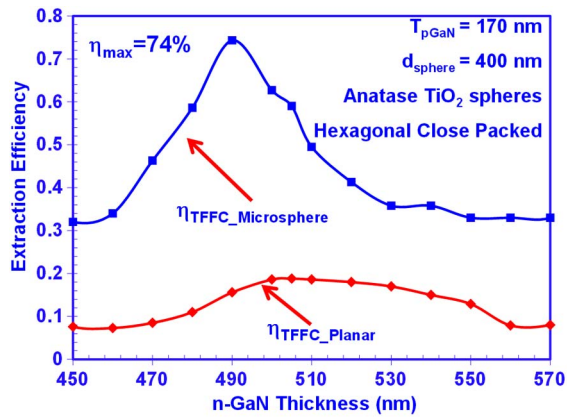


Fig. 9. Cavity-dependent light extraction efficiency of TFCC LEDs with microsphere arrays.

The TFCC LED structure was further optimized by tuning the quantum well position. The p-GaN thickness was varied from 140 to 190 nm. As shown in Fig. 10, the extraction efficiency increases first and then decreases. A maximum extraction efficiency of 75% is achieved at a p-GaN thickness of 160 nm. The light extraction efficiencies of planar TFCC LEDs with the same p-GaN thickness and cavity thickness are also plotted in Fig. 10 for comparison purposes. While the planar TFCC LEDs display a similar efficiency trend with respect to the p-GaN thickness, the overall efficiency is much lower than that of the TFCC LEDs with microsphere arrays. The notable improvement in light extraction for TFCC LEDs with microsphere arrays is attributed to the cavity effect and light–sphere interaction.

The light emitted from the quantum well is isotropic, and the forward-traveling light interferes with the totally reflected light from the metallic mirror attached to the bottom of the p-GaN layer. Constructive interference occurs when optical length difference between the forward-traveling light and reflected light equals an integer of the wavelength. The optical length difference depends on the cavity thickness and light

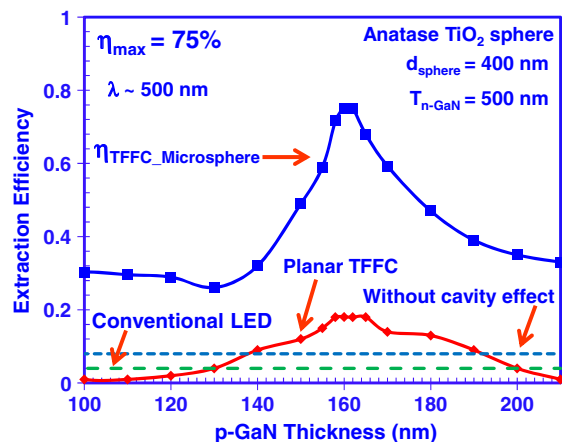


Fig. 10. p-GaN thickness-dependent light extraction efficiency of TFCC with microsphere arrays.

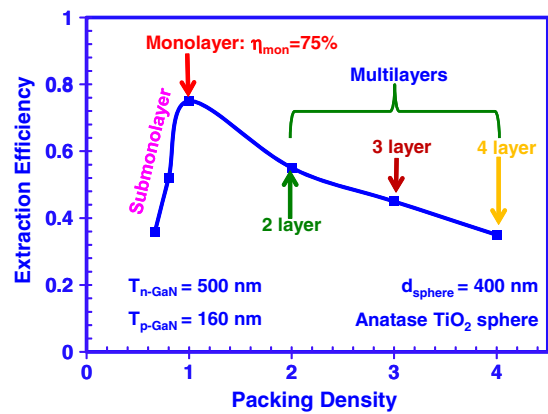


Fig. 11. Extraction efficiency of microsphere TFCC LEDs with various packing densities.

emission direction. Thus, the quantum well position and cavity thickness have a significant effect on light emission from the LED. The optimum light extraction efficiency is achieved by tuning the p-GaN and cavity thicknesses.

Further study was performed to confirm the optimization of light extraction efficiency of microsphere array TFCC LEDs by considering all the effects of microsphere packing geometry, microsphere packing density, sphere diameter, and cavity thickness. Figure 11 shows the light extraction efficiency of microsphere array TFCC LEDs with various packing densities and with optimized sphere diameter, microsphere packing geometry, and cavity thickness. Note that the packing density is presented by the ratio of the sphere diameter to the lattice period (denoted as R_d/p). For example, the hexagonal close-packed monolayer sphere array has an R_d/p of 1. The submonolayer has R_d/p smaller than 1, while the multilayer has R_d/p larger than 1. Light extraction efficiency increased with the increase in R_d/p and a maximum light extraction efficiency of 75% is achieved when a monolayer of microsphere is used on the LED. This ensures that the optimization of the light extraction efficiency of microsphere array TFCC LEDs is achieved.

5. CONCLUSION

The FDTD method was employed to calculate the light extraction efficiency of thin-film flip-chip LEDs with TiO_2 -based microsphere arrays. The cavity thickness and quantum well position were tuned to achieve optimum light extraction. In addition, the effect of periodical arrangement of sphere on light extraction was also investigated. Specifically, the light extraction efficiency of TiO_2 microsphere array LEDs with different packing densities and different packing geometries are compared. The optimized light extraction efficiency can be achieved with a hexagonal close-packed monolayer of TiO_2 sphere arrays. The use of a hexagonal close-packed monolayer of TiO_2 microsphere arrays in TFCC LEDs is expected to result in 75% light extraction efficiency, which corresponds to 3.6 times enhancement over that for optimized planar TFCC LEDs.

Funding. Daniel E. '39 and Patricia M. Smith Endowed Chair Professorship; National Science Foundation (NSF) (ECCS-1408051, CBET-1120399); U.S. Department of Energy (NETL, DE-PS26-08NT00290).

Acknowledgment. The authors also would like to acknowledge useful discussions with Wei Sun and Chee-Keong Tan, both from Lehigh University.

REFERENCES

- H. P. Maruska and J. J. Tietjen, "Preparation and properties of vapor-deposited single-crystalline GaN," *Appl. Phys. Lett.* **15**, 327–329 (1969).
- S. Nakamura, Y. Harada, and M. Seno, "Novel metalorganic chemical vapor-deposition system for GaN growth," *Appl. Phys. Lett.* **58**, 2021–2023 (1991).
- S. Nakamura, T. Mukai, M. Senoh, and N. Iwasa, "Thermal annealing effects on P-type Mg-doped GaN films," *Jpn. J. Appl. Phys.* **31**, L139–L142 (1992).
- S. Nakamura, S. J. Pearton, and G. Fasol, *The Blue Laser Diode: The Complete Story* (Springer Verlag, 2000).
- S. Nakamura, T. Mukai, and M. Senoh, "High-brightness InGaN/AlGaIn double-heterostructure blue-green-light-emitting diodes," *J. Appl. Phys.* **76**, 8189–8191 (1994).
- S. Nakamura, T. Mukai, and M. Senoh, "Candela-class high-brightness InGaN/AlGaIn double-heterostructure blue-light-emitting diodes," *Appl. Phys. Lett.* **64**, 1687–1689 (1994).
- D. A. Steigerwald, J. C. Bhat, D. Collins, R. M. Fletcher, M. O. Holcomb, M. J. Ludowise, P. S. Martin, and S. L. Rudaz, "Illumination with solid state lighting technology," *IEEE J. Sel. Top. Quantum Electron.* **8**, 310–320 (2002).
- H. Kim, S. J. Park, and H. Hwang, "Effects of current spreading on the performance of GaN-based light-emitting diodes," *IEEE Trans. Electron Devices* **48**, 1065–1069 (2001).
- X. A. Cao, E. B. Stokes, P. Sandvik, N. Taskar, J. Kretchmer, and D. Walker, "Optimization of current spreading metal layer for GaN/InGaIn-based light emitting diodes," *Solid State Electron.* **46**, 1235–1239 (2002).
- D. L. Hibbard, S. P. Jung, C. Wang, D. Ullery, Y. S. Zhao, H. P. Lee, W. So, and H. Liu, "Low resistance high reflectance contacts to p-GaN using oxidized Ni/Au and Al or Ag," *Appl. Phys. Lett.* **83**, 311–313 (2003).
- J. J. Wierer, D. A. Steigerwald, M. R. Krames, J. J. O'Shea, M. J. Ludowise, G. Christenson, Y.-C. Shen, C. Lowery, P. S. Martin, S. Subramanya, W. Götz, N. F. Gardner, R. S. Kern, and S. A. Stockman, "High-power AlGaInN flip-chip light-emitting diodes," *Appl. Phys. Lett.* **78**, 3379–3381 (2001).
- O. B. Shchekin, J. E. Epler, T. A. Trottier, T. Margalith, D. A. Steigerwald, M. O. Holcomb, P. S. Martin, and M. R. Krames, "High performance thin-film flip-chip InGaIn-GaN light-emitting diodes," *Appl. Phys. Lett.* **89**, 071109 (2006).
- J. J. Wierer, A. David, and M. M. Megens, "III-nitride photonic-crystal light-emitting diodes with high extraction efficiency," *Nat. Photonics* **3**, 163–169 (2009).
- E. Matioli and C. Weisbuch, "Impact of photonic crystals on LED light extraction efficiency: approaches and limits to vertical structure designs," *J. Phys. D* **43**, 354005 (2010).
- H. Benisty, H. De Neve, and C. Weisbuch, "Impact of planar micro-cavity effects on light extraction—Part I: basic concepts and analytical trends," *IEEE J. Quantum Electron.* **34**, 1612–1631 (1998).
- H. Benisty, H. De Neve, and C. Weisbuch, "Impact of planar micro-cavity effects on light extraction—Part II: selected exact simulations and role of photon recycling," *IEEE J. Quantum Electron.* **34**, 1632–1643 (1998).
- M. R. Krames, O. B. Shchekin, R. Mueller-Mach, G. O. Mueller, Z. Ling, G. Harbers, and M. G. Craford, "Status and future of high-power light-emitting diodes for solid-state lighting," *J. Disp. Technol.* **3**, 160–175 (2007).
- K. H. Li, K. Y. Zang, S. J. Chua, and H. W. Choi, "III-nitride light-emitting diode with embedded photonic crystals," *Appl. Phys. Lett.* **102**, 181117 (2013).
- P. Zhao and H. Zhao, "Analysis of light extraction efficiency enhancement for thin-film-flip-chip InGaIn quantum wells light-emitting diodes with GaN micro-domes," *Opt. Express* **20**, A765–A776 (2012).
- L. Han, T. A. Piedimonte, and H. Zhao, "Experimental exploration of the fabrication of GaN microdome arrays based on a self-assembled approach," *Opt. Mater. Express* **3**, 1093–1100 (2013).
- P. Kumnorkaew, Y. K. Ee, N. Tansu, and J. F. Gilchrist, "Investigation of the deposition of microsphere monolayers for fabrication of microlens arrays," *Langmuir* **24**, 12150–12157 (2008).
- X. H. Li, P. F. Zhu, G. Y. Liu, J. Zhang, R. B. Song, Y. K. Ee, P. Kumnorkaew, J. F. Gilchrist, and N. Tansu, "Light extraction efficiency enhancement of III-nitride light-emitting diodes by using 2-D close-packed TiO₂ microsphere arrays," *J. Disp. Technol.* **9**, 324–332 (2013).
- Y. K. Ee, R. A. Arif, N. Tansu, P. Kumnorkaew, and J. F. Gilchrist, "Enhancement of light extraction efficiency of InGaIn quantum wells light emitting diodes using SiO₂/polystyrene microlens arrays," *Appl. Phys. Lett.* **91**, 221107 (2007).
- Y. K. Ee, P. Kumnorkaew, R. A. Arif, H. Tong, H. P. Zhao, J. F. Gilchrist, and N. Tansu, "Optimization of light extraction efficiency of III-Nitride LEDs with self-assembled colloidal-based microlenses," *IEEE J. Sel. Top. Quantum Electron.* **15**, 1218–1225 (2009).
- X. H. Li, R. B. Song, Y. K. Ee, P. Kumnorkaew, J. F. Gilchrist, and N. Tansu, "Light extraction efficiency and radiation patterns of III-nitride light-emitting diodes with colloidal microlens arrays with various aspect ratios," *IEEE Photon. J.* **3**, 489–499 (2011).
- P. F. Zhu, G. Y. Liu, J. Zhang, and N. Tansu, "FDTD analysis on extraction efficiency of GaN light-emitting diodes with microsphere arrays," *J. Disp. Technol.* **9**, 317–323 (2013).
- Y. K. Ee, P. Kumnorkaew, R. A. Arif, H. Tong, J. F. Gilchrist, and N. Tansu, "Light extraction efficiency enhancement of InGaIn quantum wells light-emitting diodes with polydimethylsiloxane concave microstructures," *Opt. Express* **17**, 13747–13757 (2009).
- W. H. Koo, W. Youn, P. Zhu, X.-H. Li, N. Tansu, and F. So, "Light extraction of organic light emitting diodes by defective hexagonal-close-packed array," *Adv. Funct. Mater.* **22**, 3453 (2012).
- P. F. Zhu and N. Tansu, "Effect of packing density and packing geometry on light extraction of III-nitride light-emitting diodes with microsphere arrays," *Photon. Res.* (to be published).
- L.-C. Feng, K.-H. Chung, C.-C. Hsin, Y.-P. Chen, and W.-Y. Yeh, "Structural effects on highly directional far-field emission patterns of GaN-based micro-cavity light-emitting diodes with photonic crystals," *J. Lightwave Technol.* **28**, 2881–2889 (2010).
- A. Kastler, "Atomes à l'intérieur d'un Interféromètre Perot-Fabry," *Appl. Opt.* **1**, 17–24 (1962).
- W. Lukosz, "Theory of optical-environment-dependent spontaneous-emission rates for emitters in thin-layers," *Phys. Rev. B* **22**, 3030–3038 (1980).
- G. B. Friedmann and H. S. Sandhu, "Phase changes on reflection from a metallic surface," *Am. J. Phys.* **56**, 270–273 (1988).
- D. G. Deppe and C. Lei, "Spontaneous emission and optical gain in a Fabry-Perot microcavity," *Appl. Phys. Lett.* **60**, 527–529 (1992).
- H. De Neve, J. Blondelle, P. Van Daele, P. Demeester, R. Baets, and G. Borghs, "Recycling of guided mode light emission in planar microcavity light emitting diodes," *Appl. Phys. Lett.* **70**, 799–801 (1997).
- D. Delbeke, R. Bockstaele, P. Bienstman, R. Baets, and H. Benisty, "High-efficiency semiconductor resonant-cavity light-emitting diodes: a review," *IEEE J. Sel. Top. Quantum Electron.* **8**, 189–206 (2002).
- Y. C. Shen, J. J. Wierer, M. R. Krames, M. J. Ludowise, M. S. Misra, F. Ahmed, A. Y. Kim, G. O. Mueller, J. C. Bhat, S. A. Stockman, and P. S. Martin, "Optical cavity effects in InGaIn/GaN quantum-well-heterostructure flip-chip light-emitting diodes," *Appl. Phys. Lett.* **82**, 2221–2223 (2003).
- K. J. Vahala, "Optical microcavities," *Nature* **424**, 839–846 (2003).

39. H. Y. Ryu, "Modification of the light extraction efficiency in micro-cavity vertical InGaN light-emitting diode structures," *J. Korean Phys. Soc.* **55**, 1267–1271 (2009).
40. K. S. Daskalakis, P. S. Eldridge, G. Christmann, E. Trichas, R. Murray, E. Iliopoulos, E. Monroy, N. T. Pelekanos, J. J. Baumberg, and P. G. Savvidis, "All-dielectric GaN microcavity: strong coupling and lasing at room temperature," *Appl. Phys. Lett.* **102**, 101113 (2013).
41. B. G. Prevo and O. D. Velev, "Controlled, rapid deposition of structured coatings from micro- and nanoparticle suspensions," *Langmuir* **20**, 2099–2107 (2004).
42. P. Zhu, H. Zhu, W. Qin, C. K. Tan, and N. Tansu, "Eu³⁺-doped TiO₂ nanospheres for GaN-based white light-emitting diodes," in *Proc. of the SPIE Optics + Photonics Conf.*, San Diego, California, 2014.